Journal of the Mechanical Behavior of Biomedical Materials 85 (2018) 181–187

Contents lists available at ScienceDirect

Journal of the Mechanical Behavior of Biomedical Materials

journal homepage: www.elsevier.com/locate/jmbbm

Features of the volume change and a new constitutive equation of hydrogels under uniaxial compression

Y.R. Zhang[a,d], K.J. Xu[a], Y.L. Bai[a,c], L.Q. Tang[a,b,*], Z.Y. Jiang[a], Y.P. Liu[a], Z.J. Liu[a], L.C. Zhou[a], X.F. Zhou[d]

[a] School of Civil Engineering and Transportation, South China University of Technology, No.381, Wushan Road, Guangzhou, Guangdong, China
[b] State Key Laboratory of Subtropical Building Science, South China University of Technology, No.381, Wushan Road, Guangzhou, Guangdong, China
[c] LNM, Institute of Mechanics, Chinese Academy of Sciences, Beijing, China
[d] Guangdong Institute of Intelligent Manufacturing, Guangzhou, China

ARTICLE INFO

Keywords:
Constitutive equation
Volume change
Hydrogel

ABSTRACT

For high-water content hydrogels in compression, the water inside of hydrogels contributes to the response of hydrogels to external loads directly, but part of the water is expelled from hydrogels in the meantime to change the volume of the hydrogel and reduce the contribution. In order to consider the contribution of the water in the constitution equation, PVA (polyvinyl alcohol) hydrogels with high-water content were used as examples, and compressive experiments were carried out to measure both the stress-strain relation and the change of the volume in the meantime. By considering the effect of the difference of the contribution of water in different directions of the hydrogel, we deduced a new constitutive equation, which can pretty well depict the stress-strain of hydrogels with different water contents. The results showed that the contribution of water to the total stress increases with the compression strain and even exceed that of the polymer, although the expelled water reduces the contribution at the early loading stage, which well explains the difference of elastic moduli of hydrogels in compression and tension.

1. Introduction

Polymeric hydrogels are promising soft materials in tissue engineering and medicine; that consist of continuous polymerized network structures that can absorb and retain a large amount of water (Baker et al., 2012; Hodge et al., 2015; Kobayashi and Oka, 2004; Oyen, 2013). For tissue engineering applications, the mechanical properties of hydrogels, especially their compressive performance are critical (Curley et al., 2014; Gofman and Buyanov, 2017; Hayes et al., 2016; Kanca et al., 2018; Tingting et al., 2017). The water content of hydrogels can be higher than 90% and even up to 99.7% (Appel et al., 2012; Si et al., 2017), and water is one of the significant factors that causes the hydrogel to respond differently in tension and compression. Polyvinyl alcohol (PVA) hydrogels with about 80% water content are shown in Fig. 1, and the tensile curve is more nonlinear than the compression curve. This is mainly due to the greater change in fiber alignment during the stretching (Dong et al., 2017). Even under small deformation ($< 5\%$), the tension elastic modulus (about 0.15 MPa) of the hydrogel is smaller than the compression modulus (about 0.25 MPa). Within such a small deformation, the tensile and the compressive responses of the polymer network should be similar. Thus, what making the difference between tension and compression in the hydrogel only be the water inside the hydrogel. The water may resist compression but not tension.

The high-water content of hydrogels is one of the key factors that contributes to their excellent biocompatibility and resemblance of living tissues (Ovsianikov et al., 2011; Van Vlierberghe et al., 2011). Free water in hydrogels with high-water content can be expelled out of the specimen under compression, which means that the volume will change even in air (Frensemeier et al., 2010; Milimouk et al., 2001; Nakamura et al., 2001; Urayama et al., 2008; Urayama and Takigawa, 2012; Vervoort et al., 2005; Zhang et al., 2017); therefore, it is necessary to measure the change of volume induced by the expelled water in compression. Most compressive constitutions of hydrogels were summarized phenomenologically from experiment (Kaufman et al., 2008; Korchagin et al., 2007; Sasson et al., 2012; Święszkowski et al., 2006) without considering the effect of expelled water. Professor Suo and his team considered the change of Helmholtz free energy generated by the polymer network stretching and the surrounding environment, and proposed a set of equations of state in which the changes of hydrogel volume were included (Cai and Suo, 2012; Faghihi et al., 2014; Hong

* Corresponding author at: School of Civil Engineering and Transportation, South China University of Technology, 581 Wushan Road, Guangzhou, Guangdong, China.
E-mail address: lqtang@scut.edu.cn (L.Q. Tang).

https://doi.org/10.1016/j.jmbbm.2018.06.004
Received 23 April 2018; Received in revised form 26 May 2018; Accepted 2 June 2018
Available online 05 June 2018
1751-6161/

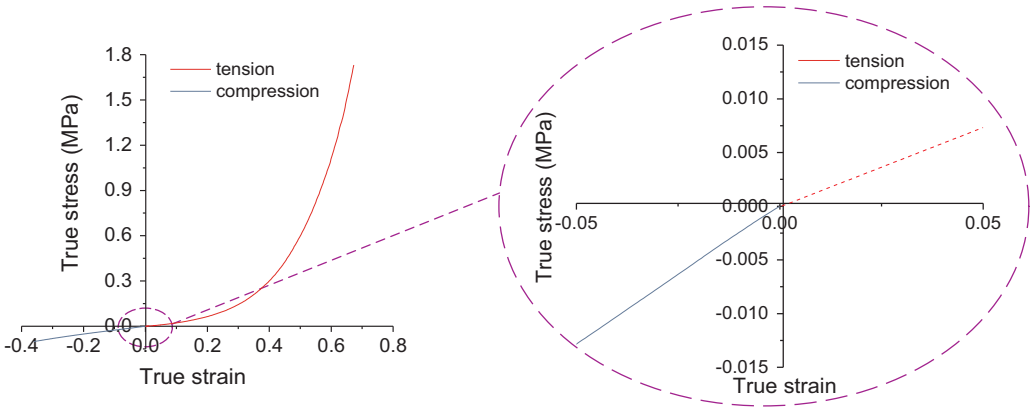

Fig. 1. The difference of the tensile and compressive properties of the PVA hydrogel with about 80% water content.

et al., 2008; Hong et al., 2009; Hong et al., 2010; Li et al., 2014; Marcombe et al., 2010). In these models, the contributions of water are directly related to the change of volume of water, which means that the water's contributions to hydrogel stresses are the same in all directions. However, such an assumption is questionable when the deformation of the hydrogel is large.

To study the contribution of water, the volume change should be measured first. Although the measurement of expelled water from hydrogels is very difficult, several researchers have reported experiments. Urayama et al. (2008), Urayama and Takigawa (2012) and Vervoort et al. (2005) measured the volume loss by digital image processing and obtained the correlation between the loss amount and some experimental conditions such as loading rate, water content of specimens and boundary friction. These experiments with digital image methods have great reference value, but there are still some technical difficulties for measuring the volume changes of hydrogels: hydrogels are so soft that the samples may not maintain their revolving shape, and the semi-transparency may blur the specimen boundaries.

In this paper, we used high-water content PVA hydrogels as examples to study the volume change behaviour under compression. We used experiments to measure the uniaxial stress-strain relations and the change of volume. The volume measurements used a digital image-based system in which two cameras ensured the volumes of the specimens under axisymmetrical deformations. Furthermore, to distinguish the contributions of the polymer network and the water of hydrogels in compression, we deduced a constitutive equation considering the different contributions of water to hydrogel stresses under different directions. The model not only explains the contributions of the polymer network and water in compression, but it also explains the differences in elastic moduli of hydrogels in compression and tension.

2. Method

2.1. Experiment

2.1.1. Sample preparation

The mixture of PVA powder (SIGMA-ALDRICH, Mw 89000–98000) and deionized water was maintained at 110 °C in an autoclave for approximately 5 h. The mass of water was decided according to the desired water content of the mixture. The viscous aqueous PVA solution was poured into moulds and subjected to 6 cycles between −25 °C and 25 °C, and each period was 12 h. The height of samples was 30 mm, and the diameter was also 30 mm. Fig. 2(a) is a photo of three samples with different water contents, and Fig. 2(b) is their remaining polymer after drying. The exact initial water content c_w of each specimen was determined by a drying test after the compressive experiment,

$$c_w = \frac{m_{whole} - m_{dry}}{m_{whole}} \quad (1)$$

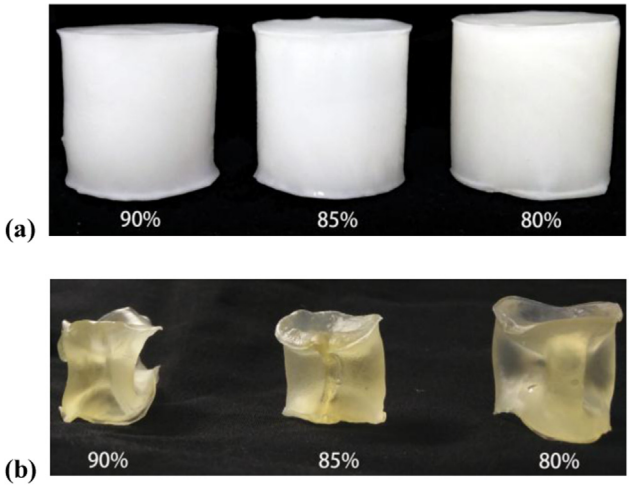

Fig. 2. Photos of the sample: (a) three PVA hydrogel samples with different water content: 90%, 85% and 80%. (b) The remaining polymer after drying the samples.

where m_{whole} is the mass of the sample, and m_{dry} is the remaining mass after drying.

2.1.2. Volume measurement

Digital image processing can evaluate the volume variation (or Poisson's ratio) during loading without contact (Baghereih et al., 2008; Chen et al., 2013; Pritchard et al., 2013; Urayama et al., 1993). We also used this technique to measure the volume change of the hydrogels. As mentioned above, soft specimens may deform unexpectedly during loading. Thus, calculation methods using a revolving column become inapplicable. Therefore, the deformations need to be monitored and such specimens should be removed. Besides, the sharpness of the specimen contour is crucial to the reliability of the experimental results, but the translucence of PVA hydrogels decreases photo clarity. To solve these two problems, we used two cameras to record deformation from different directions concurrently. We used fluorescent powder to cover the specimen surface so that the self-luminous specimens contrast strongly with a dark background (Fig. 3). Imaging data are sufficient to calculate the volume of a revolving body, and the second camera can monitor whether the specimen has shear or other unexpected deformation. The dark environment can be achieved with a large carton. More details of the experimental method are introduced in Appendix I.

2.1.3. Testing system

The two SLR (single lens reflex) cameras were Canon 80D (EF-S 18–200 mm f/3.5–5.6 IS) and Sony α55 (DT 3.5–5.6/18–55 SAM). The

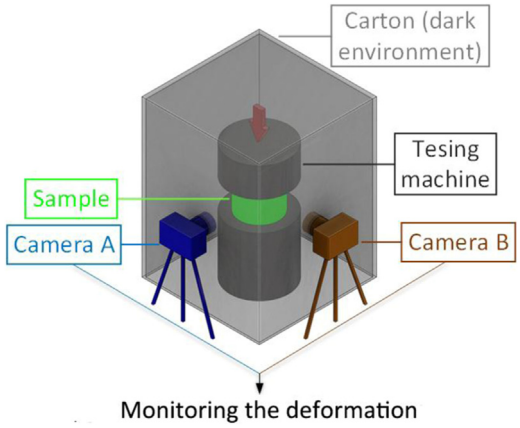

Fig. 3. Schematic diagram of the experimental method.

testing machine used in this paper was made by CARE (model M-100, China) with a loading system driven by electromagnets. The compressive loading strain rate was 0.1%/s (0.03 mm/s). To reduce the friction between the specimen and the testing machine, the upper and lower surfaces of the sample were coated with lubricating oil. An initial photo was taken before loading, and photos were taken every 3 s as the specimen was being compressed.

2.2. Theoretical model

Fig. 4(a) illustrates a hydrogel block. In the initial state, the block is a unit cube subjecting to no applied forces. In the current state, the hydrogel is subject to axial applied forces and has a true stress tensor $\boldsymbol{\sigma}$.

The stress of the hydrogel combines the contributions of the polymer network and the water.

$$\boldsymbol{\sigma} = \boldsymbol{\sigma}^p + \boldsymbol{\sigma}^w \tag{2}$$

where $\boldsymbol{\sigma}^p$ and $\boldsymbol{\sigma}^w$ are tensors that reflect the contributions of the polymer network and the water in the true stress tensor of the hydrogel respectively. We used $\mathbf{F}$ to represent the deformation gradient tensor with stretch in three coordinate directions. The normalized cross-sectional areas (comparing to initial area) against three coordinates are A_x, A_y, and A_z respectively. The normalized areas of the three cross sections are also contributed by the polymer and the water (Fig. 4(b)):

$$\begin{aligned} A_x &= A_x^p + A_x^w \\ A_y &= A_y^p + A_y^w \\ A_z &= A_z^p + A_z^w \end{aligned} \tag{3}$$

Here, A_x^p and A_x^w are two normalized area of polymer and the water in the cross section of x axis. Terms A_y^p, A_y^w, A_z^p and A_z^w, have similar meanings.

We first consider the polymer network. For elastic material, the Cauchy (true) stress depends on the strain energy and the deformation gradient (Volokh, 2016). In this case we have

$$\boldsymbol{\sigma}^p = \frac{\mathbf{F}^T}{J} \cdot \frac{\partial W^p}{\partial \mathbf{F}} \tag{4}$$

where W^p is the strain energy of the polymer network, and J is the normalized volume of the hydrogel so there is $J = \det(\mathbf{F})$. If the temperature is defaulted without change and no shearing deformation occurs, then the strain energy can be calculated as (Wall and Flory, 1951)

$$W^p = \frac{\kappa \upsilon}{2}[\alpha_1^2 + \alpha_2^2 + \alpha_3^2 - 3 - 2\ln(\alpha_1\alpha_2\alpha_3)] \tag{5}$$

where κ is the Boltzmann constant (about $1.38 \times 10^{\hat{}-23}$ J/K), υ is the number of chains in the network, α_1, α_2 and α_3 are principle stretches. For hydrogels with only axial strain, we insert Eq. (5) in Eq. (4) and have

$$\begin{aligned} \sigma_x^p &= \frac{\kappa \upsilon}{J}(\alpha_x^2 - 1) \\ \sigma_y^p &= \frac{\kappa \upsilon}{J}(\alpha_y^2 - 1) \\ \sigma_z^p &= \frac{\kappa \upsilon}{J}(\alpha_z^2 - 1) \end{aligned} \tag{6}$$

where σ_x^p, σ_y^p and σ_z^p are the stress components contributed by polymer in coordinate directions.

We used σ_{static}^w to represent the "hydrostatic pressure" of water in the hydrogel. Although "hydrostatic pressure" is the same in all directions, the components in the stress tensor $\boldsymbol{\sigma}^w$ are different. This is because the effective normalized area A_x^w is not equal to the normalized area A_x in the x direction. It also changes with strain, which is similar to other two directions. The water stresses in the three main directions are equal to the following:

$$\begin{aligned} \sigma_x^w &= \sigma_{static}^w \cdot A_x^w \\ \sigma_y^w &= \sigma_{static}^w \cdot A_y^w \\ \sigma_z^w &= \sigma_{static}^w \cdot A_z^w \end{aligned} \tag{7}$$

Inserting Eq. (6) and Eq. (7) in Eq. (2), we have

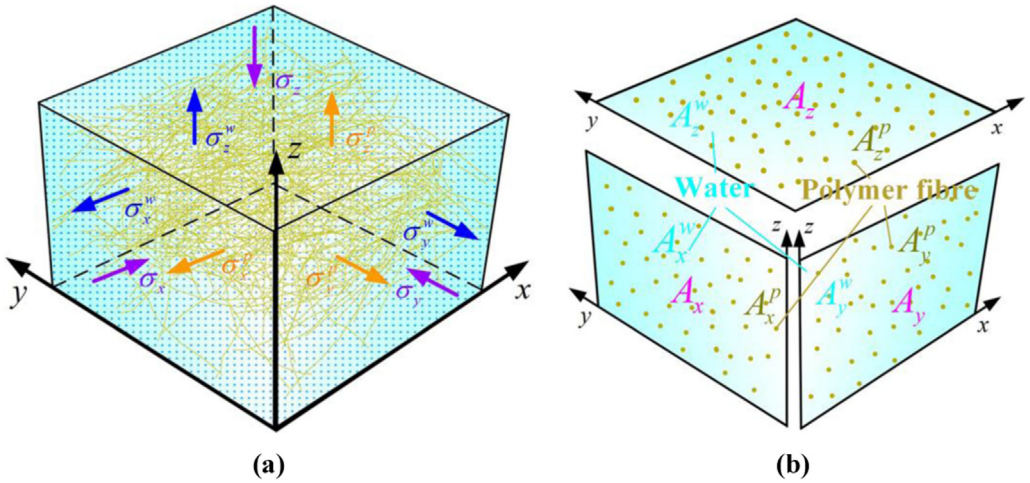

Fig. 4. A unit volume of a hydrogel subjected to only axial forces: (a) the total stress is contributed by both the polymer and the water; (b) the area of the three cross sections are also contributed by the polymer and the water.

$$\sigma_x = \frac{\kappa\upsilon}{J}(\alpha_x^2 - 1) + \sigma_{static}^w \cdot A_x^w$$
$$\sigma_y = \frac{\kappa\upsilon}{J}(\alpha_y^2 - 1) + \sigma_{static}^w \cdot A_y^w$$
$$\sigma_z = \frac{\kappa\upsilon}{J}(\alpha_z^2 - 1) + \sigma_{static}^w \cdot A_z^w \tag{8}$$

For uniaxial compression, there is $\sigma_x = \sigma_y = 0$, $\alpha_x = \alpha_y$ (z is set as the loading direction), $A_x^w = A_y^w$ and $J = \alpha_x\alpha_y\alpha_z$, so Eq. (8) converts into

$$0 = \frac{\kappa\upsilon}{J}\left(\frac{J}{\alpha_z} - 1\right) + \sigma_{static}^w \cdot A_x^w$$
$$\sigma_z = \frac{\kappa\upsilon}{J}(\alpha_z^2 - 1) + \sigma_{static}^w A_z^w \tag{9}$$

Combining the two equations in Eq. (9), we obtained

$$\sigma_z = \frac{\kappa\upsilon}{J}\left[(\alpha_z^2 - 1) + \frac{A_z^w}{A_x^w}\left(1 - \frac{J}{\alpha_z}\right)\right] \tag{10}$$

The definition of the stretch and the true strain are

$$\alpha_z = \frac{l_z}{l_z^0} \tag{11}$$

$$\varepsilon_z = \int \frac{\delta l_z}{l_z} \tag{12}$$

where l_z^0 and l_z are the initial length and the current length of the hydrogel in z direction. Thus, the relationship between the stretch and the true strain is

$$\alpha_z = e^{\varepsilon_z} \tag{13}$$

Using the true strain replaces the stretch, Eq. (10) changes into

$$\sigma_z = \frac{\kappa\upsilon}{J}[e^{2\varepsilon_z} - 1 + \frac{A_z^w}{A_x^w}(1 - Je^{-\varepsilon_z})] \tag{14}$$

In each cross section, the area A_i, A_i^w (i = 1,2,3 to representative x, y, z) will change with the deformation ε_z. Obviously, A_z^w will increase but A_x^w will decrease with increasing ε_z. Thus, A_z^w/A_x^w will have an incremental relation of the deformation ε_z. Here we simply let $A_z^w/A_x^w = k\varepsilon_z + 1$ (k is a parameter depends on the material). Eq. (14) then changes into:

$$\begin{aligned}\sigma_z &= \frac{\kappa\upsilon}{J}[e^{2\varepsilon_z} - 1 + (k\varepsilon_z + 1)(1 - Je^{-\varepsilon_z})] \\ &= \frac{\kappa\upsilon}{J}(e^{2\varepsilon_z} + k\varepsilon_z - Je^{-\varepsilon_z} - kJ\varepsilon_z e^{-\varepsilon_z})\end{aligned} \tag{15}$$

Eq. (15) is established for high-water content hydrogels under uniaxial compression load. Due to the water expulsive behaviour, the hydrogel stress is not only related to the strain, but also related to the volume change. The parameter υ will take different values for diverse hydrogels.

The contributions of the polymer and the water is expressed as Eq. (16) and Eq. (17), respectively.

$$\sigma_z^p = \frac{\kappa\upsilon}{J}(e^{2\varepsilon_z} - 1) \tag{16}$$

$$\sigma_z^w = \frac{\kappa\upsilon}{J}(k\varepsilon_z + 1)(1 - Je^{-\varepsilon_z}) \tag{17}$$

In the above derivation, both deformation and stress are positive for tension and negative for compression.

3. Results and discussion

3.1. Monitoring axisymmetrical deformation of specimens

Fig. 5(a) shows the photos of a sample obtained from the two cameras under several strains. If the deformations of the two groups were roughly the same, then the experiment was regarded as effective. Fig. 5(b) shows the comparison of the experimental results obtained from the two cameras. Only if the two curves were approximately the same in the range of errors, the experimental data were believed reliable. If the experimental results do not satisfy these two conditions, then we can conclude that the specimen did not remain as a revolving body during uniaxial compression.

3.2. True stress against the strain with water content

Fig. 6(a) shows the true stress-strain curves with three different initial water contents. True strain is the integral of each infinitesimal deformation divided by the length, and true stress is the force divided by the actual cross-sectional area undergoing loading (Young, 1989). The use of engineering strain and engineering stress will cause significant errors due to the large deformation and the large Poisson's ratio close 0.5 of the hydrogels (Karimi et al., 2014). That is why we used true stress and true strain. The water content has a remarkable effect on the mechanical properties of hydrogels, and accurate measurements of the initial water content are necessary to reduce experimental error. That is why we tested the initial water content for each sample. Under the same strain, reducing the initial water content can greatly improve the stress of the samples. However, it is worth noting that while both the differences in initial water content are 5%, the difference between the 80% and 85% curves is greater than that between the 85% and 90% curves. This might be due to the rise in polymer cross-linking density as the polymer content increases.

3.3. Volume change against the strain with water content

The normalized volume J is the ratio of the current volume V and the initial volume V_0.

$$J = \frac{V}{V_0} \tag{18}$$

Fig. 6(b) shows three normalized volume-strain curves with three initial water contents. The rate of volume change decreases with

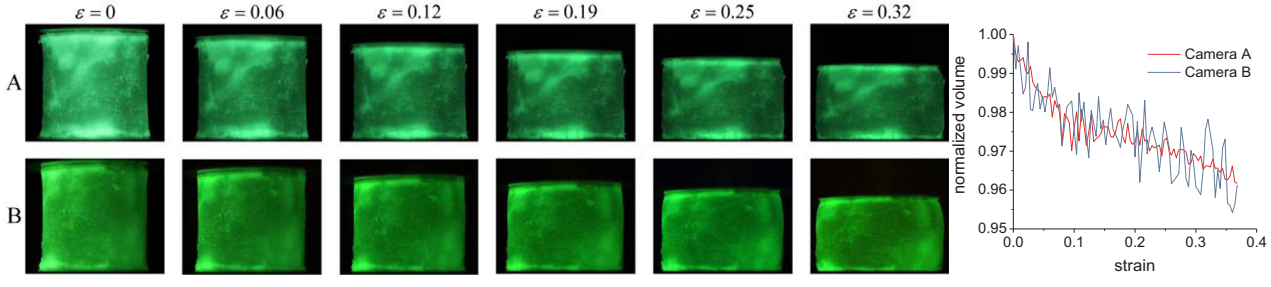

Fig. 5. Monitoring results: (a) Group A and Group B photos were obtained from two cameras from different directions at the same time; (b) The normalized volume curve obtained from these two group photos.

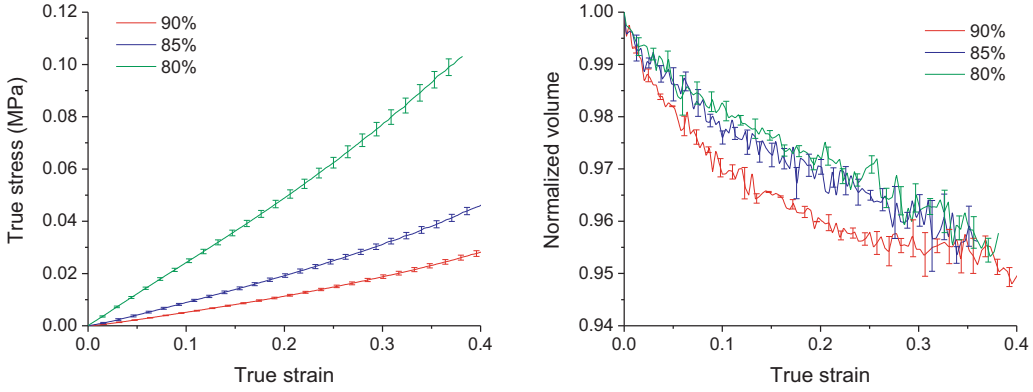

(a) (b)

Fig. 6. Experimental results of PVA hydrogels with 80%, 85%, and 90% initial water contents: (a) True stress-strain curves; (b) Normalized volume-strain curves.

increasing strain. This might be because the side surface area of the specimen will gradually decrease with increased strain—this results in less room for water passage, and slow speed of water expulsion (Urayama and Takigawa, 2012). When the strain reaches a certain value, the volume becomes stable, and this implies that most of the remaining water is retained in the specimen and bears external strain with polymer fibres. This trend was particularly obvious for samples with 90% water content.

For ease of characterization, we used simple functions to fit the curves in Fig. 6(b) and the results were as Eq. (19).

$$\begin{aligned} &90\%: \quad J = 1 - 0.075\varepsilon^{0.42} \\ &85\%: \quad J = 1 - 0.079\varepsilon^{0.58} \\ &80\%: \quad J = 1 - 0.080\varepsilon^{0.63} \end{aligned} \tag{19}$$

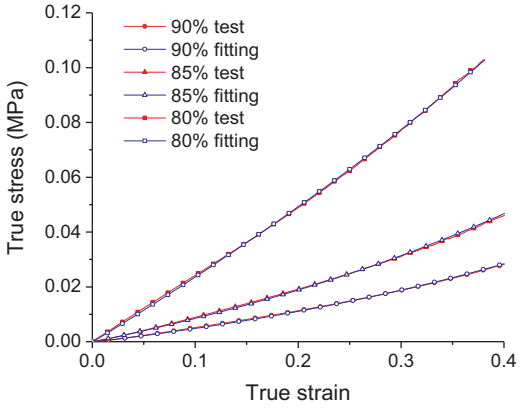

Fig. 7. The fitting curves of Eq. (15).

3.4. Contributions of polymer and water in the stress of hydrogel

By convention, the tensile value is positive while that of compression is negative. However, in uniaxial compression tests, for convenience, all of the compressive results are generally considered positive. Therefore, the experimental true stress σ and strain ε have a relationship with the stress and strain in Eq. (15) as $\sigma = -\sigma_z$, and $\varepsilon = -\varepsilon_z$. Constants $\kappa\upsilon$ and k can be fitted by combining our experimental data (Fig. 6(a) and Eq. (19)) and Eq. (15). The values are shown in Table 1 and the fitting curves of Eq. (15) are shown in Fig. 7. The fitting effects are very good.

From Table 1, the variations of parameters $\kappa\upsilon$ and k with water content are reasonable. Term $\kappa\upsilon$ indicates the amount of polymer in the unit volume of the hydrogel. It increases with decreasing water content; k reflects the contribution of water to the stress of hydrogel, and it increases with increasing water content.

Eq. (16) and Eq. (17) are the effects of polymer and water, respectively. Their changes with strain are shown in Fig. 8(a-c). The contribution of water to the total stress increases with strain, which is opposite that of the rate of volume change. The contribution of water will exceed the polymer if the strain is large enough, although the contribution of the polymer is several times larger than that of water at early stage.

While the contribution of water is several times lower than that of the polymer network at the early stage of loading process (strain less than 0.05), there are obvious errors if this is neglect throughout. In the Introduction, we suggested that the compression elastic modulus is larger than the tension one because the water plays a role in the compressive progress, but it cannot directly resist tensile deformation. That is, the compression and the tension elastic modulus should be the same without the effect of water. To verify this view, the front of the curve with 80% water content is magnified, and the corresponding stress of the polymer network is drawn (Fig. 8(d)). The compression elastic modulus here is 0.24 MPa and the slope of the polymer stress curve is 0.17 MPa. These are close to the experimental results (0.25 MPa and 0.15 MPa). The closeness of the total stress curve is not surprise because it is a fitting curve. However, the similarity between the tension modulus and the slope of the compressive polymer curve is an interesting result, and it confirmed that the water is what makes the hydrogel compression elastic modulus greater than the tension one.

To further understand the effect of expelled water on the total stress, we suppose there was no volume change ($J = =1$) in the stress-strain relation shown in Eq. (15), and thus:

$$\sigma_z = \kappa\upsilon(e^{2\varepsilon_z} + k\varepsilon_z - e^{-\varepsilon_z} - k\varepsilon_z e^{-\varepsilon_z}) \tag{20}$$

Fig. 9 shows the comparison of Eq. (15) with Eq. (20). As expected, the presence of water expulsion decreases the total stress. Using curves with 90% water content as an example, the reduction of the stress is approximately 5% when there is water expulsion. Hydrogels can re-absorb the expelled water in a solvent environment, and they can not only relieve the applied stress but can also restore themselves *in vivo*. The water expulsion behaviour might have interesting applications.

Table 1
The parameters of PVA hydrogel with different water contents.

Water content (%)	90	85	80
Value of $\kappa\upsilon$(MPa)	0.016	0.028	0.083
Value of k	−4.04	−3.49	−1.67

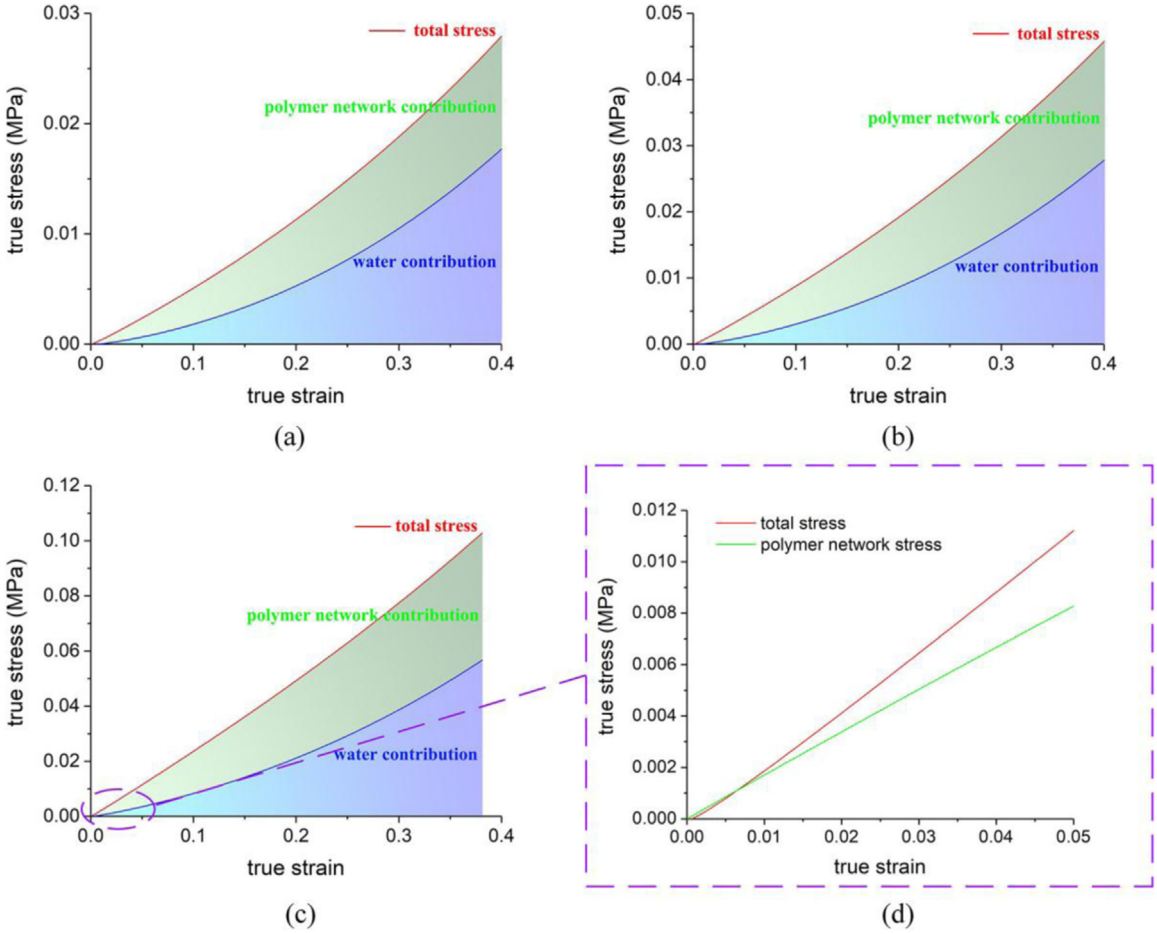

Fig. 8. Comparison of the contributions of the fiber network and water to the total stress of the whole hydrogel: (a) 90% water content; (b) 85% water content; (c) 80% water content. And (d) the front of the curve with 80% water content.

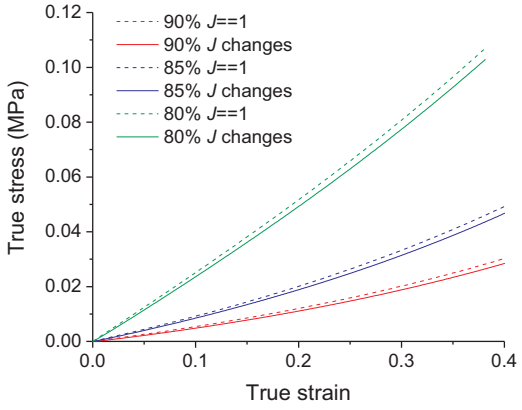

Fig. 9. Effect of water expulsion on the stress of hydrogels under compression.

4. Conclusions

We studied the change in hydrogel volume during compression and compared the properties of the volume change and stress-strain relation of high-water content hydrogels. We also deduced a constitutive equation that contains the effects of the polymer network and the water, in which the contributions of water on stresses in different direction were considered. This study draws some conclusions:

(1) With considering the effect of the difference of water on stresses of hydrogel in different directions, the new constitutive equation nicely depicts the stress-strain relation of hydrogels with different water contents.
(2) The contribution of water increases with the strain and will exceed that of the polymer if the strain is sufficiently large.
(3) The effect of water is the main cause of the difference between the elastic moduli of hydrogels in tension and compression.
(4) The volume change resulting from water expulsion may reduce the stress of the hydrogels in compression.

Acknowledgements

This work was financially supported by the National Natural Science Foundation of China (NSFC no. 11472109, 11772134) and the Natural Science Foundation of Guangdong Province (2015A030311046 and 2015B010131009).

Appendix A. Supporting information

Supplementary data associated with this article can be found in the online version at http://dx.doi.org/10.1016/j.jmbbm.2018.06.004.

References

Appel, E.A., Loh, X.J., Jones, S.T., Biedermann, F., Dreiss, C.A., Scherman, O.A., 2012. Ultrahigh-water-content supramolecular hydrogels exhibiting multistimuli responsiveness. J. Am. Chem. Soc. 134, 11767–11773.
Bagherieh, A.R., Habibagahi, G., Ghahramani, A., 2008. A novel approach to measure the volume change of triaxial soil samples based on image processing. J. Appl. Sci. 8, 2387–2395.
Baker, M.I., Walsh, S.P., Schwartz, Z., Boyan, B.D., 2012. A review of polyvinyl alcohol

and its uses in cartilage and orthopedic applications. J. Biomed. Mater. Res. Part B Appl. Biomater. 100B, 1451–1457.
Cai, S., Suo, Z., 2012. Equations of state for ideal elastomeric gels. Epl 97, 34009.
Chen, F., Kang, D.-J., Park, J.-H., 2013. New measurement method of Poisson's ratio of PVA hydrogels using an optical flow analysis for a digital imaging system. Meas. Sci. Technol. 24, 055602.
Curley, C., Hayes, J.C., Rowan, N.J., Kennedy, J.E., 2014. An evaluation of the thermal and mechanical properties of a salt-modified polyvinyl alcohol hydrogel for a knee meniscus application. J. Mech. Behav. Biomed. Mater. 40, 13–22.
Dong, S., Huang, Z., Tang, L., Zhang, X., Zhang, Y., Yi, J., 2017. A three-dimensional collagen-fiber network model of the extracellular matrix for the simulation of the mechanical behaviors and micro structures. Comput. Methods Biomech. Biomed. Eng. 20, 991–1003.
Faghihi, S., Karimi, A., Jamadi, M., Imani, R., Salarian, R., 2014. Graphene oxide/poly (acrylic acid)/gelatin nanocomposite hydrogel: experimental and numerical validation of hyperelastic model. Mater. Sci. Eng.: C 38, 299–305.
Frensemeier, M., Koplin, C., Jaeger, R., Kramer, F., Klemm, D., 2010. Mechanical properties of bacterially synthesized nanocellulose hydrogels. Macromol. Symp. 294, 38–44.
Gofman, I.V., Buyanov, A.L., 2017. Unusual effect evidenced at the investigations of the mechanical behavior of composite hydrogels under cyclic compression. J. Mech. Behav. Biomed. Mater. 71, 238–243.
Hayes, J.C., Curley, C., Tierney, P., Kennedy, J.E., 2016. Biomechanical analysis of a salt-modified polyvinyl alcohol hydrogel for knee meniscus applications, including comparison with human donor samples. J. Mech. Behav. Biomed. Mater. 56, 156–164.
Hodge, R.M., Simon, G.P., Whittaker, M.R., Hill, D.J.T., Whittaker, A.K., 2015. Free volume and water uptake in a copolymer hydrogel series. J. Polym. Sci. Part B Polym. Phys. 36, 463–471.
Hong, W., Zhao, X., Zhou, J., Suo, Z., 2008. A theory of coupled diffusion and large deformation in polymeric gels. J. Mech. Phys. Solids 56, 1779–1793.
Hong, W., Liu, Z., Suo, Z., 2009. Inhomogeneous swelling of a gel in equilibrium with a solvent and mechanical load. Int. J. Solids Struct. 46, 3282–3289.
Hong, W., Zhao, X., Suo, Z., 2010. Large deformation and electrochemistry of polyelectrolyte gels. J. Mech. Phys. Solids 58, 558–577.
Kanca, Y., Milner, P., Dini, D., Amis, A.A., 2018. Tribological properties of PVA/PVP blend hydrogels against articular cartilage. J. Mech. Behav. Biomed. Mater. 78, 36–45.
Karimi, A., Navidbakhsh, M., Alizadeh, M., Razaghi, R., 2014. A comparative study on the elastic modulus of polyvinyl alcohol sponge using different stress-strain definitions. Biomed. Tech. Biomed. Eng. 59, 439–446.
Kaufman, J.D., Miller, G.J., Morgan, E.F., Klapperich, C.M., 2008. Time-dependent mechanical characterization of poly(2-hydroxyethyl methacrylate) hydrogels using nanoindentation and unconfined compression. J. Mater. Res. 23, 1472–1481.
Kobayashi, M., Oka, M., 2004. Characterization of a polyvinyl alcohol-hydrogel artificial articular cartilage prepared by injection molding. J. Biomater. Sci.-Polym. Ed. 15, 741–751.
Korchagin, V., Dolbow, J., Stepp, D., 2007. A theory of amorphous viscoelastic solids undergoing finite deformations with application to hydrogels. Int. J. Solids Struct. 44, 3973–3997.
Li, J., Suo, Z., Vlassak, J.J., 2014. A model of ideal elastomeric gels for polyelectrolyte gels. Soft Matter 10, 2582–2590.
Marcombe, R., Cai, S., Hong, W., Zhao, X., Lapusta, Y., Suo, Z., 2010. A theory of constrained swelling of a pH-sensitive hydrogel. Soft Matter 6, 784–793.
Milimouk, I., Hecht, A.M., Beysens, D., Geissler, E., 2001. Swelling of neutralized polyelectrolyte gels. Polymer 42, 487–494.
Nakamura, K., Shinoda, E., Tokita, M., 2001. The influence of compression velocity on strength and structure for gellan gels. Food Hydrocoll. 15, 247–252.
Ovsianikov, A., Deiwick, A., Van Vlierberghe, S., Dubruel, P., Möller, L., Dräger, G., Chichkov, B., 2011. Laser fabrication of three-dimensional CAD Scaffolds from photosensitive gelatin for applications in tissue engineering. Biomacromolecules 12, 851–858.
Oyen, M.L., 2013. Mechanical characterisation of hydrogel materials. Int. Mater. Rev. 59, 44–59.
Pritchard, R.H., Lava, P., Debruyne, D., Terentjev, E.M., 2013. Precise determination of the Poisson ratio in soft materials with 2D digital image correlation. Soft Matter 9, 6037–6045.
Sasson, A., Patchornik, S., Eliasy, R., Robinson, D., Haj-Ali, R., 2012. Hyperelastic mechanical behavior of chitosan hydrogels for nucleus pulposus replacement-experimental testing and constitutive modeling. J. Mech. Behav. Biomed. Mater. 8, 143–153.
Si, Y., Wang, L., Wang, X., Tang, N., Yu, J., Ding, B., 2017. Ultrahigh-water-content, superelastic, and shape-memory nanofiber-assembled hydrogels exhibiting pressure-responsive conductivity. Adv. Mater. 29, 1700339.
Święszkowski, W., Ku, D.N., Bersee, H.E.N., Kurzydlowski, K.J., 2006. An elastic material for cartilage replacement in an arthritic shoulder joint. Biomaterials 27, 1534–1541.
Tingting, X., Wanqian, L., Li, Y., 2017. A review of gradient stiffness hydrogels used in tissue engineering and regenerative medicine. J. Biomed. Mater. Res. Part A 105, 1799–1812.
Urayama, K., Takigawa, T., Masuda, T., 1993. Poisson's ratio of poly(vinyl alcohol) gels. Macromolecules 26, 3092–3096.
Urayama, K., Taoka, Y., Nakamura, K., Takigawa, T., 2008. Markedly compressible behaviors of gellan hydrogels in a constrained geometry at ultraslow strain rates. Polymer 49, 3295–3300.
Urayama, K., Takigawa, T., 2012. Volume of polymer gels coupled to deformation. Soft Matter 8, 8017–8029.
Van Vlierberghe, S., Dubruel, P., Schacht, E., 2011. Biopolymer-based hydrogels as scaffolds for tissue engineering applications: a review. Biomacromolecules 12, 1387–1408.
Vervoort, S., Patlazhan, S., Weyts, J., Budtova, T., 2005. Solvent release from highly swollen gels under compression. Polymer 46, 121–127.
Volokh, K., 2016. Mechanics of Soft Materials. Springer, Singapore.
Wall, F.T., Flory, P.J., 1951. Statistical thermodynamics of rubber elasticity. J. Chem. Phys. 19, 1435–1439.
Young, W.C., 1989. Roark's Formulas for Stress and Strain. McGraw-Hill, United States.
Zhang, Y.R., Tang, L.Q., Xie, B.X., Xu, K.J., Liu, Z.J., Liu, Y.P., Jiang, Z.Y., Dong, S.B., 2017. A variable mass meso-model for the mechanical and water-expelled behaviors of PVA hydrogel in compression. Int. J. Appl. Mech. 09, 1750044.